이학석사 학위논문

# The study of dendritic block copolymers having cross-linkable polyisoprene blocks

## 가교 가능한 폴리아이소프렌을 소수성 블록으로 갖는 블록 공중합체 연구

2018 년 2 월

서울대학교 대학원

화학부 고분자화학 전공

윤 미 선

# The study of dendritic block copolymers having cross-linkable polyisoprene blocks

지도 교수 김 경 택

이 논문을 이학석사 학위논문으로 제출함
2018 년 2 월

서울대학교 대학원
화학부 고분자화학 전공
윤 미 선

윤미선의 이학석사 학위논문을 인준함
2018 년 2 월

위 원 장 최 태 림 (인)

부위원장 김 경 택 (인)

위 원 손 병 혁 (인)

# Abstract

## The study of dendritic block copolymers having cross-linkable polyisoprene blocks

**Misun Yoon**
**Polymer Chemistry in Department of Chemistry**
**The Graduate School**
**Seoul National University**

Block copolymers (BCPs) are macromolecules composed of two or more distinct polymer blocks joined together by covalent bonds. BCPs have been highlighted as self-assembling molecules for creating well-defined nanostructures in bulk and solution, which are potentially valuable materials for drug delivery system, catalyst carrier, and separation membrane. Well-defined mesoporous structures can be directly created by self-assembly of BCPs in solution. For the formation of well-defined porous structures by self-assembly, the architectures, molecular weight of constituting blocks, and their molecular weight ratios have to be carefully adjusted. Also, the conditions for self-assembly have to be optimized. By carefully design and synthesis of the structural components of BCPs, preferential self-assembly in solution into well-defined porous structures has been demonstrated. However, the BCPs in the well-defined nanostructures are only held by non-covalent interaction. These porous nanostructures are unable to be used under harsh environments. Therefore, it is desirable that the self-assembled mesoporous structures are covalently stabilized to resist harsh conditions such as the presence of organic solvents, high temperature, extreme pH, and

physical stress. In this thesis, I show the synthesis of block copolymers composed of a branched hydrophilic poly(ethylene glycol) (PEG) block and branched hydrophobic polyisoprene (PI). PI possesses a low glass transition temperature ($T_g$) and main-chain and pendant vinyl groups that can be used for cross-linking. I investigated the effect of architecture and block ratio of these BCPs on their self-assembly behaviors in solution. The covalent stabilization of the self-assembled structures of these block copolymers was carried out by cross-linking of PI blocks. The effect of the cross-linking of the PI domain on the structural stability of the nanostructure was investigated under harsh conditions.

**Keyword :** block copolymer, Poly(ethylene glycol), Polyisoprene, solution self-assembly, cross-linking, nanostructure

**Student Number :** 2016-20353

# Table of Contents

# List of Figures, Schemes, and Tables

## Figures

## Schemes

# Tables

# 1. Introduction

Recently, block copolymers (BCPs) have been highlighted as promising materials to create porous polymer films having pores of precisely defined size and spatial arrangement. BCP is a type of copolymer which is made up of different homopolymer blocks. BCPs have various architectures such as linear, cyclic, branched, bottlebrush, and miktoarm. BCPs undergo microphase separation because of immiscibility of constituting polymer blocks.

Amphiphilic BCPs self-assemble into micellar and vesicular aggregates in a block-selective solvent. A block-selective solvent only dissolves one of the polymer blocks constituting the BCP. The shape of the self-assembled structures obtained by solution self-assembly of BCPs are determined by the architecture of BCPs, expressed by critical packing parameter *P*. Molecular packing parameter theory was developed to describe the relationship between the chemical structure of an amphiphilic lipid and the morphology of its self-assembled structure[1-2]. And the morphological transition of self-assembled structures of BCPs in solution was also successfully rationalized by it.[3-5]The critical packing parameter *P* is defined as $P = V/a_0 l_c$ where $V$ is the volume of the hydrophobic block, $a_0$ is the area of the hydrophilic block, and $l_c$ is the length of the hydrophobic block.[6-7] By increasing the *P* value, spherical micelle structure was favored for $P < 1/3$, cylindrical structure for $1/3 < P < 1/2$, vesicle structure for $1/2 < P < 1$, lamellar structure for $P = 1$ and inverse phase for $1 < P$.[3, 8-14]

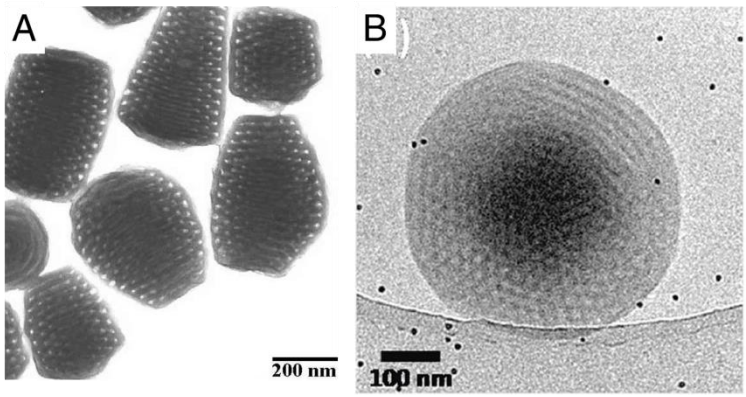


**Figure 1**. (A)TEM image of hexagonal hollow shape from solution self-assembly of $PAA_{13}$-*b*-$PS_{400.}$ Eisenberg *et al*. Reprinted image from Ref 15. (B) Cryo-TEM image of polymer cubosome from self assembly of bottlebruss-like $PEO_{39}$-*b*-$PODMA_{17.}$ Sommerdijk *et al*. Reprinted image from Ref 16.

The structural analogy between a BCP and a lipid suggests that the high asymmetry of the architecture of the BCP should warrant its *P* value to be greater than unity, which might result in the preferential self-assembly into inverse mesophases in solution. Eisenberg and coworkers[3, 9, 15] reported that the self-assembly of a diblock copolymer, poly(acrylic acid)-b-polystyrene (PAA-b-PS) having highly asymmetric architecture, self-assembled in solution into nanopaticles having internal hexagonal hollow hoops (HHHs). Holder and Sommerdijk[16-18] reported the formation of polymer cubosomes, analogues to colloidally stabilized nanoparticles of lipid cubic mesophases (cubosomes), via solution self-assembly from amphiphilic BCPs having hydrophobic blocks of bottlebrush-like architectures.

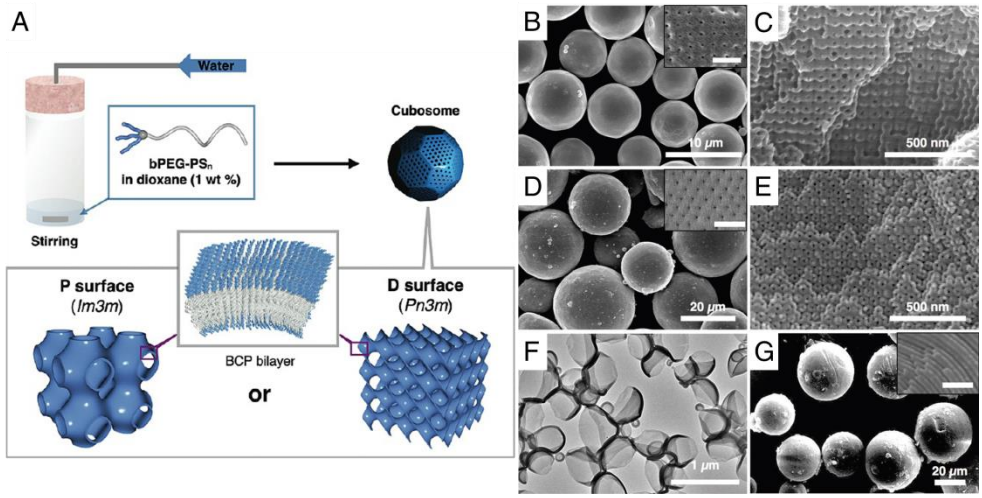


**Figure 2**. (A)Schemetic illustration of self-assembly of dendritic-linear PEG-*b*-PS into polymer cubosomes consisting of an inverse bicontinuous cubic crystalline structure of block copolymer bilayers. An *et al*. Reprinted image from Ref 11. B-E) SEM images of the polymer cubosomes of (B, C) $PEG550_3$-$PS_{211}$ showing *Im3m* structure and (D, E) $PEG550_3$-$PS_{231}$ showing *Pn3m* structure. (The inset scale bars: 200 nm). (F) TEM image of the polymersomes of $PEG550_3$-$PS_{177}$. (G) SEM image of the hexasomes of $PEG550_3$-$PS_{283}$ showing the HII structure (The inset scale bar: 200 nm). La *et al*. Reprinted image from Ref 12.

Recently, bicontinuous inverse cubic mesophases were observed from direct solution self-assembly of BCPs with non-linear architecture such as dendritic-linear shapes.[10-12] The dendritic architecture of the hydrophilic block ensured that the overall molecular weight of the hydrophilic PEG domain remained unchanged, while the area of the hydrophilic block was increased by multiplying the number of peripheral chains. When these dendritic hydrophilic blocks were combined with a hydrophobic PS block,

the resulting dendritic-linear BCPs could self-assemble into colloidal particles composed of inverse cubic mesophases of the BCP bilayers in solution. Furthermore, the branched hydrophobic domain might render the *P* value of the BCP to be increased due to a decrease in the critical chain length of the hydrophobic domain. The structural factors of the BCP contribution to the increase of the *P* value of a BCP was pronounced when the branched architecture was introduced to the hydrophobic polymer block without altering the molecular weight of the polymer blocks and the block ratio of the BCP.[13]

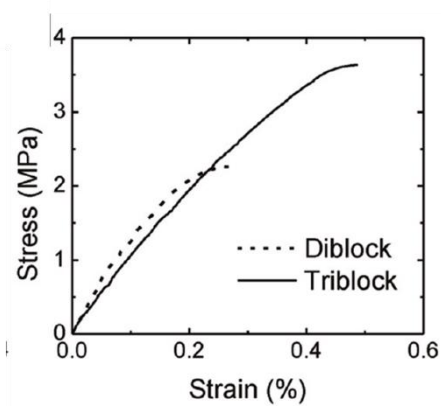


**Figure 3.** Stress-strain curve of the bulk poly(isoprene-*b*-styrene-*b*-4-vinyl pyridine) triblock terpolymer and poly(styrene-*b*-4-vinyl pyridine) diblock copolymer films. Philips *et al*. Reprinted image from Ref 19.

Direct self-assembly of BCPs into inverse bicontinuous cubic mesophases provides colloidal particles and monolithic films possessing cubic crystalline networks of water channels. These materials could pave a way to create mesoporous materials having a long path length for separation along the reticulated of water channels having a controlled diameter and surface functionality. For this purpose, the physical properties of the porous

materials should be well-controlled to resist chemical and physical stresses such as solvents, extreme temperature and pH, and mechanical force. When BCPs are composed of glassy hydrophobic polymer blocks such as polystyrene, the resulting mesoporous materials might lack the toughness required to provide robust films under pressure. Philips et al. [19] reported graded mesoporous hybrid films formed by self-assembly of triblock terpolymers containing polyisoprene as a soft hydrophobic block. The presence of hydrophobic polymers having a low glass transition temperature might provide a means of controlling the mechanical properties of the resulting block copolymers and their self-assembled nanostructures. The control of the mechanical properties of the self-assembled structures can be further optimized by covalent stabilization of the continuous domain consisting of the hydrophobic polymer blocks.

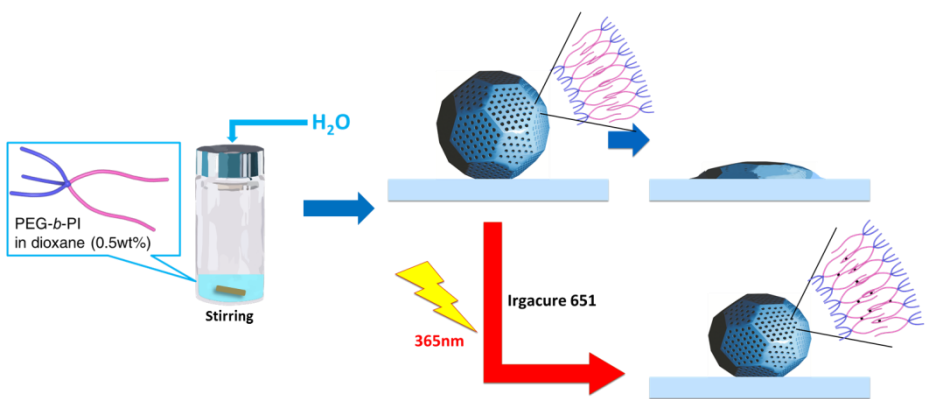


**Figure 4.** Schematic illustration of the study of dendritic block copolymers having cross-linkable rubbery hydrophobic blocks

In this thesis, I describe the synthesis of BCPs having polyisoprene (PI) as a hydrophobic polymer block for increasing the mechanical property of

the assembled structure. Polyisoprene is an amorphous polymer having low glass transition temperature ($T_g$ = -60 ~ -10 ℃). PI was anionically polymerized using synthesized alkyllithium initiator. The branched hydrophilic PEG block was synthesized by alkylation of PEG chains to the aromatic core, which was subsequently coupled with the focal units having azide groups at the desired locations. I adopted Cu(I)-catalyzed azide-acetylene ‘click chemistry’ to join the hydrophilic and hydrophobic block. The synthesized BCPs were self-assembled in solution. The morphology of assembled structures was studied by cryogenic-TEM due to the low $T_g$ of the PI blocks. The relationship between the structure of the BCP and its self-assembly was used to rationalize the transformation of morphology. Utilizing the presence of unsaturated bonds in the backbone and pendants, the PI blocks could be covalently cross-linked to form three-dimensional networks by radical coupling.[20-21] The cross-linked colloidal particles and graded films could be interesting porous materials for separation due to the improved mechanical properties arising from the rubber-like PI domains.

# 2. Results and discussion

## Synthesis of structural modules and block copolymers.

### Synthesis of hydrophobic modules

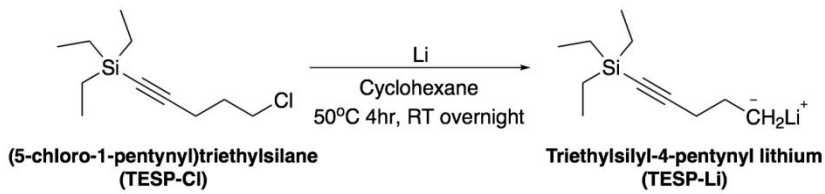


**Scheme 1.** Lithiation of (5-chloro-1-pentynyl)triethylsilane (TESP-Cl) to 5-Triethylsilyl-4-pentynyl lithium (TESP-Li).

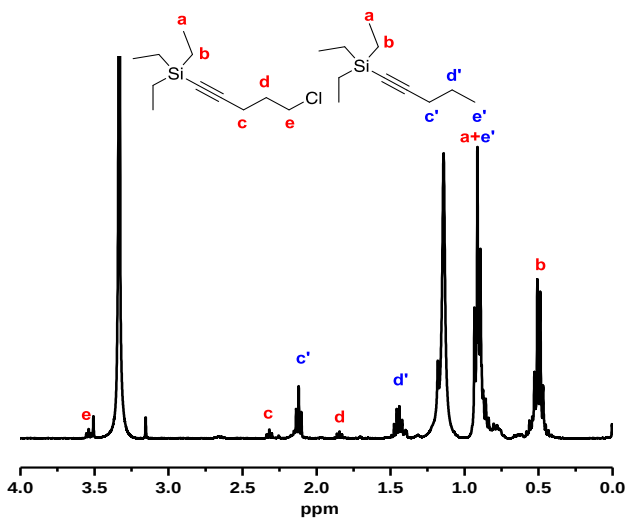


**Figure 5**. $^{1}$H NMR spectrum of TESP-Li after quenching with methanol ($CDCl_3$). Impurity peaks at 3.49 ppm and 1.09 ppm were methanol.

In general, anionic living polymerization of isoprene was initiated by sec-

butyllithium.[22-23] However, I synthesized the alkyl lithium initiator containing protected acetylene functional group for making acetylene functionalized PI. 5-Triethylsilyl-4-pentynyllithium (TESP-Li) was synthesized by reacting TESP-Cl with lithium to afford the alkynyl lithium compound (Scheme 1).[24] The degree of lithiation was estimated by $^{1}$H NMR integration after quenching the compound with methanol (Figure 5). Figure 3 showed that the ~ 60% of TESP-Cl was converted to the corresponding alkynyl lithium TESP-Li. The synthesized alkyl lithium (TESP-Li) was used as an initiator for living anionic polymerization. By using the functional alkyl lithium as an initiator, the presence of the desired functional group, α-acetylene group, at the end of the polymer chain should be guaranteed.

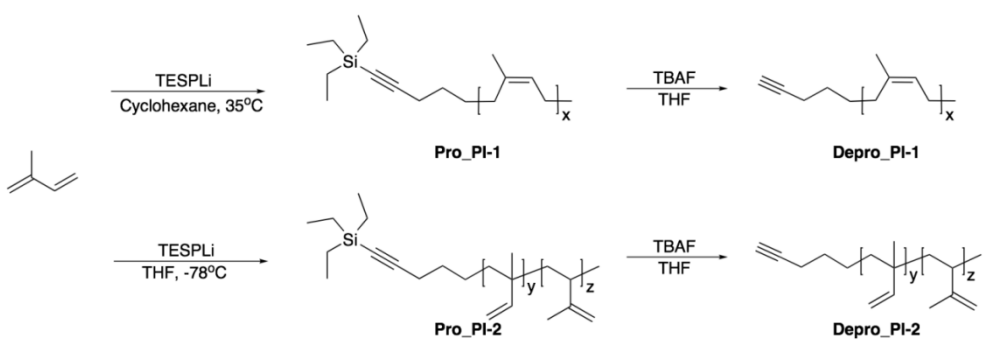


**Scheme 2.** Anionic polymerization of isoprene; Pro-1 mainly consisted of cis-1,4-addition microstructures. Pro-2 mainly consisted of 1,2 and 3,4-addition microstructures.

**Table 1**. Characterization of Polyisoprene (PI)

| Entry | Sample | $M_n$ (g mol$^{-1}$)[a] | Đ[a] | $DP_n$ (PI)[b] | 1,4- : 1,2- : 3,4-[c] | contour length (nm)[d] |
|---|---|---|---|---|---|---|
| **PI 1** | $PI_{82}$ | 5560 | 1.16 | 82 | 95 : 0 : 5 | 49 |
| **PI 2** | $PI_{214}$ | 14600 | 1.08 | 214 | 94 : 0 : 6 | 128 |
| **PI 3** | $PI_{225}$ | 15300 | 1.22 | 225 | 93 : 0 : 7 | 134 |
| **PI 4** | $PI_{495}$ | 33500 | 1.32 | 492 | 94 : 0 : 6 | 294 |
| **PI 5** | $PI^*_{154}$ | 10500 | 1.09 | 154 | 0 : 38 : 62 | 47 |

[a] The number-average molecular weight and molecular weight distribution determined by GPC (THF, 35, 0.3ml min$^{-1}$ flow rate ) using PS standards. [b] The number-average degree of polymerization ($DP_n$) of the PI block determined by $^1$H NMR integration. [c] The ratio of the PI microstructure determined by $^1$H NMR integration. PI* contained 1,2- and 3,4-rich-isoprene structure. [d] Contour length = # of polymer backbone C-C bond × 1.54 (Å) , # of the polymer backbone C-C bond is calculated according to the ratio of PI microstructure ( 4 for 1,4- and 2 for 1,2- and 3,4- ).

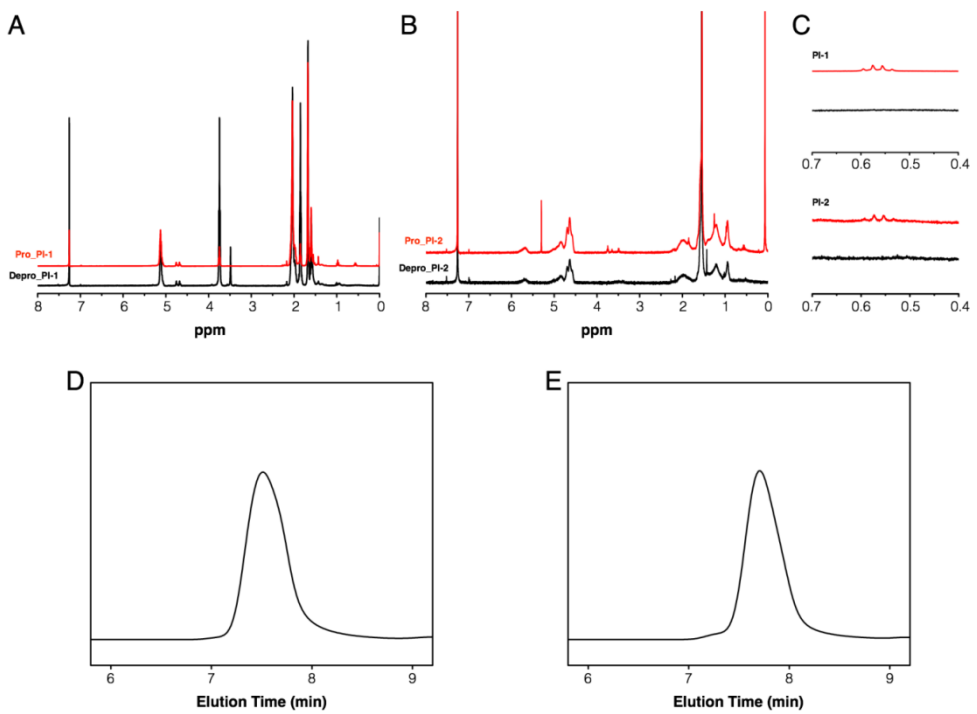

**Figure 6.** A-B) Representative $^{1}H$ NMR ($CDCl_3$) spectra of (A) Pro_PI-1(Red) and Depro_PI-1(Black) of **PI 2** polymer and (B) Pro_PI-2(Red) and Depro_PI-2(Black) of **PI 5** polymer. (C) Enlarged $^{1}H$ NMR spectra of A, B for confirming the deprotection. The disappearance of TES proton peak (-$CH_2$-, q, 0.55ppm) D-E) Representative gel permeation chromatography spectra of (D) Depro_PI-1 **PI 2** and (E) Depro_PI-2 **PI 5** polymer.

For hydrophobic blocks, I anionically polymerized isoprene with triethylsilyl-protected pentynyl lithium as an initiator. The propagation rate of anionic polymerization is dependent on the polarity of the solvent.[25-26] In polar solvent, propagation rate is proportionally increased to the increasing degree of the polarity of the solvent, which can be summarized by the Winstein spectrum.[27] Polymerization was conducted in cyclohexane for 2h at 35 ℃, which predominantly produced PI having 1,4-*cis* microstructures along the PI backbone. When the polymerization was carried out in THF at -78 ℃, the 1,2-rich microstructure with pendant vinyl group along the PI backbone was obtained. [23] By altering the microstructure of the PI backbone, I adjusted the contour length of the PI chain. The resulting PI chains were analyzed by $^{1}H$ NMR and GPC (Figure 6), which showed well-defined microstructures and molecular weight distribution (Table 1). The TES protecting group was removed by reacting the resulting PI with tetrabutylammonium fluoride (TBAF), resulting in PI chains with acetylene end group. The complete deprotection of TES was confirmed by $^{1}H$-NMR (Figure 6C). The region of NMR spectrum peak depended on the microstructures of PI.

**Synthesis of hydrophilic modules** [28, 29]

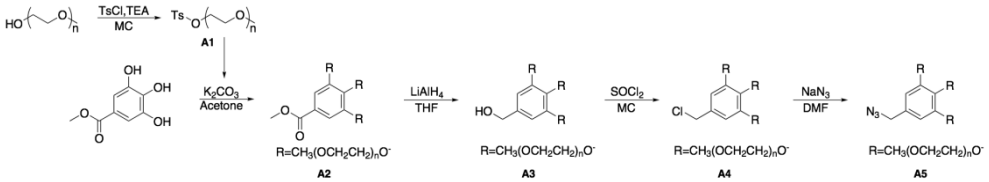


**Scheme 3.** Synthesis of dendritic PEG module which was hydrophilic domain.

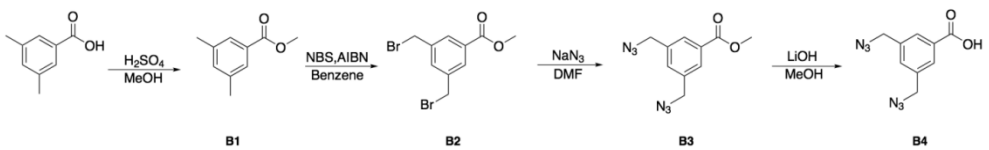


**Scheme 4.** Synthesis of methyl 3,5-bis(azidomethyl)benzoic acid which was hydrophilic module bridge.

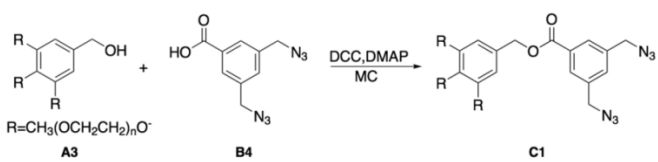


**Scheme 5.** Synthesis of $PEG750_3$-bisazide using Stiglich esterification.

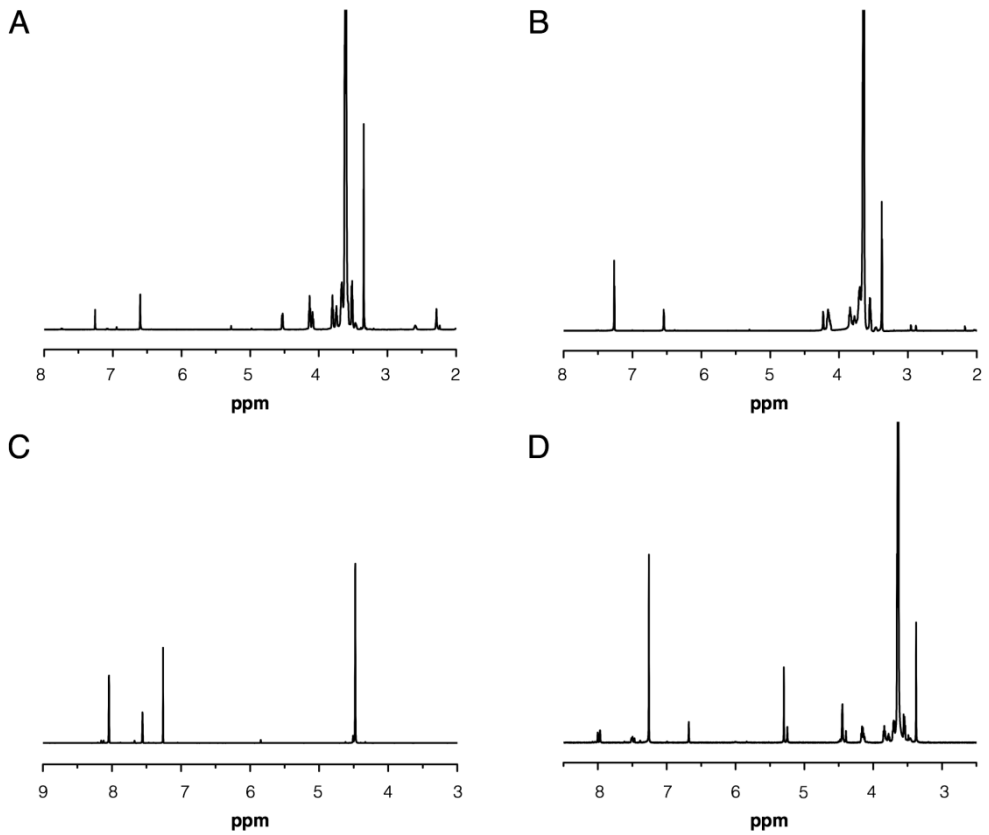


**Figure 7**. A-D) $^{1}H$ NMR ($CDCl_3$) spectra of (A) $PEG750_3$-benzyl alcohol **(A3)**, (B) $PEG750_3$-azide **(A5)**, (C) Methyl 3,5-bis(azidomethyl)benzoic acid **(B4)**, and (D) $PEG750_3$-bisazide **(C1)**.

The branched PEG block was synthesized by alkylation of oligo(ethylene glycol) chains to the methyl 3,4,5-trihydroxybenzoate core, followed by reduction of the focal methyl ester into the hydroxymethyl group (**A3**) (Scheme 3). To this core, 3,5-azidomethylbenzoic acid (**B4**) (Scheme 4) was reacted by the Stiglich esterification, which yielded the hydrophilic structural modules having the desired number of azide groups at the predetermined locations (Scheme 5). Branched PEG block with one azide group (**A5**) was synthesized by chlorination of the compound A3, followed

by substitution with $NaN_3$. Successful synthesis of each product was confirmed by $^1H$ NMR (Figure 7).

**Synthesis of block copolymers by click chemistry**

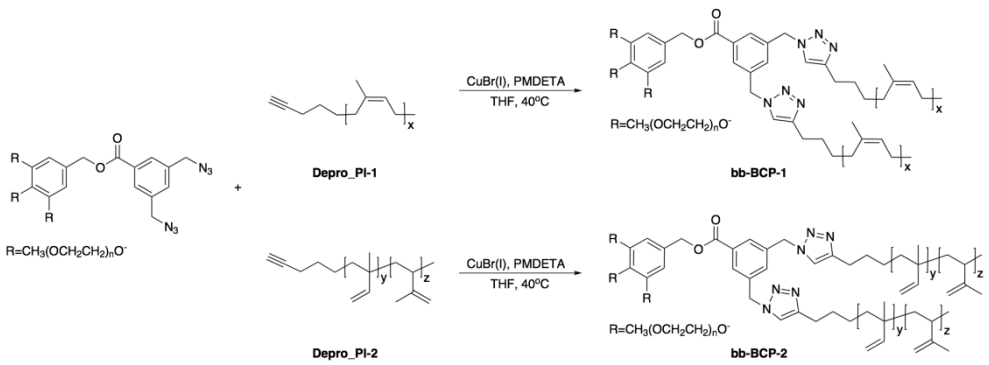


**Scheme 6.** Click chemistry of dendritic PEG module with two PI blocks; PI of bb-BCP-1 mainly consisted of cis-1,4-addition microstructures. PI of bb-BCP-2 mainly consisted of 1,2 and 3,4-addition microstructures.

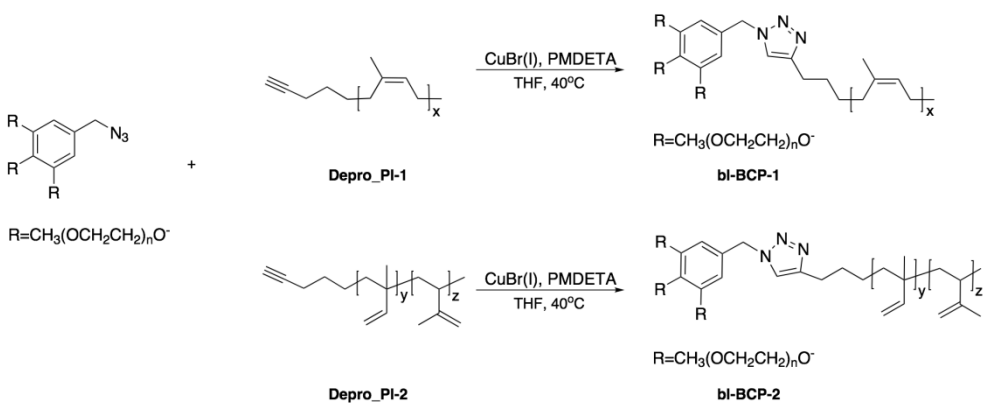


**Scheme 7.** Click chemistry of dendritic PEG module with one PI blocks; PI of bl-BCP-1 mainly consisted of cis-1,4-addition microstructures. PI of bl-BCP-2 mainly consisted of 1,2 and 3,4-addition microstructures.

**Table 2**. Characterization of PEG-*b*-PI Branched Block Copolymers

| Entry | Sample | $M_n$ (g mol$^{-1}$)[a] | Đ[a] | $DP_n$ (PI)[b] | $f_{PEG}$ (%)[c] | contour length (nm)[d] |
|---|---|---|---|---|---|---|
| **BCP 1** | $PEG750_3$-*b*-$(PI_{82})_2$ | 17000 | 1.12 | 82 | 13.2 | 49 |
| **BCP 2** | $PEG750_3$-*b*-$(PI_{214})_2$ | 28800 | 1.14 | 214 | 7.8 | 128 |
| **BCP 3** | $PEG550_3$-*b*-$(PI_{225})_2$ | 24900 | 1.29 | 225 | 6.6 | 134 |
| **BCP 4** | $PEG550_3$-*b*-$PI_{495}$ | 29800 | 1.23 | 492 | 5.5 | 294 |
| **BCP 5** | $PEG750_3$-*b*-$(PI^*_{154})_2$ | 20300 | 1.16 | 154 | 11.0 | 47 |

[a] The number-average molecular weight and molecular weight distribution determined by GPC (THF, 35, 0.3ml min$^{-1}$ flow rate ) using PS standards. [b] The number-average degree of polymerization ($DP_n$) of the PI block determined by $^1$H NMR integration. [c] The molecular weight ratio of the hydrophilic PEG domain ($f_{PEG}$) to that of the hydrophobic PI block (2250 for $PEG750_3$ and 1650 g mol$^{-1}$ for $PEG550_3$ ). PI* contained 1,2- and 3,4-rich-isoprene structure. [d] Contour length = # of polymer backbone C-C bond × 1.54 (Å) , # of the polymer backbone C-C bond is calculated according to the ratio of PI microstructure ( 4 for 1,4- and 2 for 1,2- and 3,4- ).

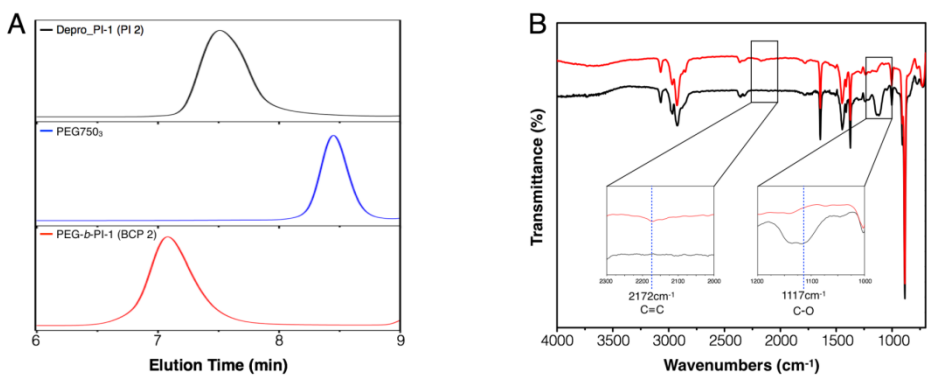


**Figure 8.** (A) Representative gel permeation chromatography (GPC) spectra showing the molecular weight change after click reaction of bb-BCP-1 **BCP 2**. (B) Fourier transform infrared (FT-IR) spectra showing changes after click reaction between **PI 5** (red) and **BCP 5** (black). The carbon-carbon

triple bond peak at 2172 $cm^{-1}$. Carbon-oxygen ether bond peak at 1117 $cm^{-1}$.

The hydrophilic and hydrophobic structural modules were joined to form BCPs by Cu(I)-catalyzed azide-alkyne click chemistry in THF. The progress of the click reaction was monitored by GPC. After confirming completion of the reaction by GPC, the resulting BCP was purified by repeated precipitation in methanol and following column chromatography. GPC spectrum of clicked BCP showed 28.8kg $mol^{-1}$ which is the sum of the each of blocks molecular weight; 2.28kg $mol^{-1}$ of one PEG block and 14.6kg $mol^{-1}$ of two PI blocks (Figure 8A). The GPC spectrum confirmed the complete conversion of the click product by showing a unimodal peak of the corresponding product. FT-IR spectrum also confirmed the completion of click reaction by the disappearance of the stretching band of the alkyne triple bond of the PI at 2172 $cm^{-1}$ (Figure 8B). FT-IR spectrum of the BCP showed the presence of C-O stretching band at 1117 $cm^{-1}$, which suggested the successful conjugation of the hydrophilic and hydrophobic blocks by the click reaction.

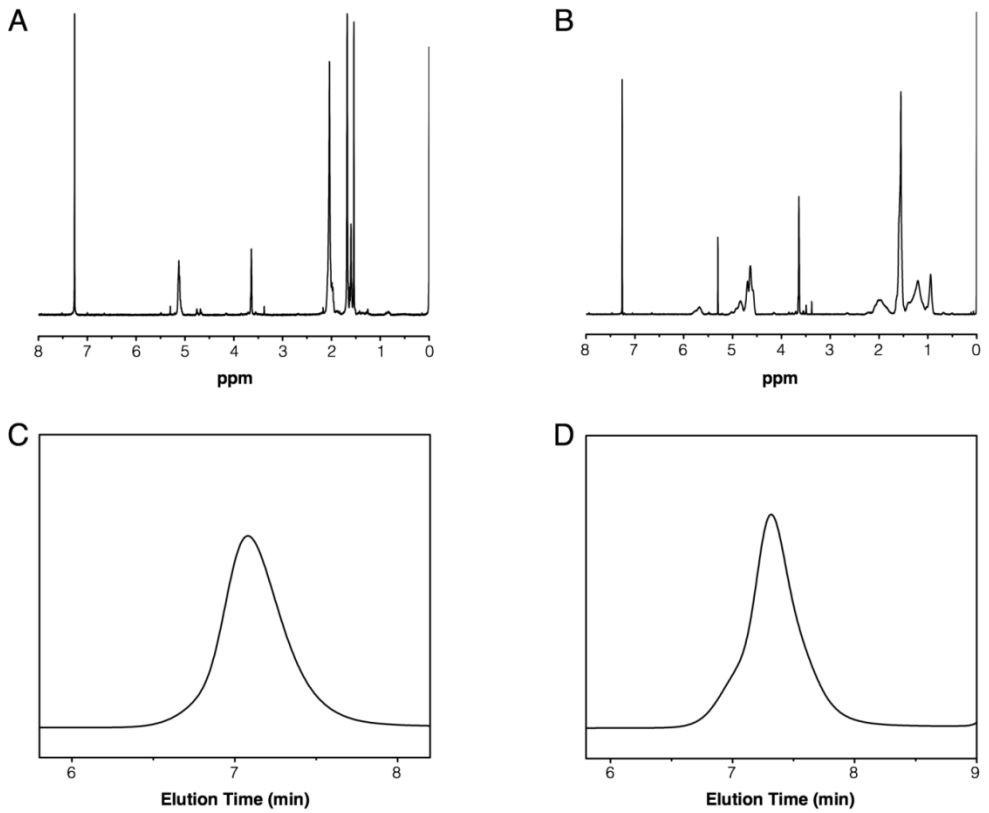


**Figure 9.** A-B) Representative $^{1}H$ NMR ($CDCl_3$) spectra of (A) bb-BCP-1 **BCP 2** and (B) bb-BCP-2 **BCP 5** polymer. C-D) Representative GPC spectra of (C) bb-BCP-1 **BCP 1** and (D) bb-BCP-2 **BCP 5** polymer.

The resulting BCP was confirmed by $^{1}H$-NMR and GPC (Figure 9). NMR spectrum of purified BCP showed both hydrophilic PEG block peaks from 3 ppm to 4 ppm and hydrophobic PI block peaks from 0.8 ppm to 2 ppm and from 4.5 ppm to 6 ppm. Spectrum shape was differed by microstructures of PI. The integration ratio of PEG and PI corresponded to the molecular weight ratio of each block. The molecular weights of BCPs were measured by GPC and each unimodal spectrum corresponded to the sum of PEG and PI blocks molecular weight.

## Solution self-assembly of dendritic PEG-*b*-PI.

I investigated the solution self-assembly of the various combination of dendritic PEG-*b*-PI (Table 2). These BCPs were diluted in dioxane (2mL, 0.5wt% ) and self-assembled by adding the same volume of water (2mL) at a regulated rate (1mL $hr^{-1}$) with stirring. Dialysis against water was followed. All the self-assembly of BCPs was under the same condition for comparison. Morphology was observed through cryogenic-TEM due to the low glass transition temperature of PI.

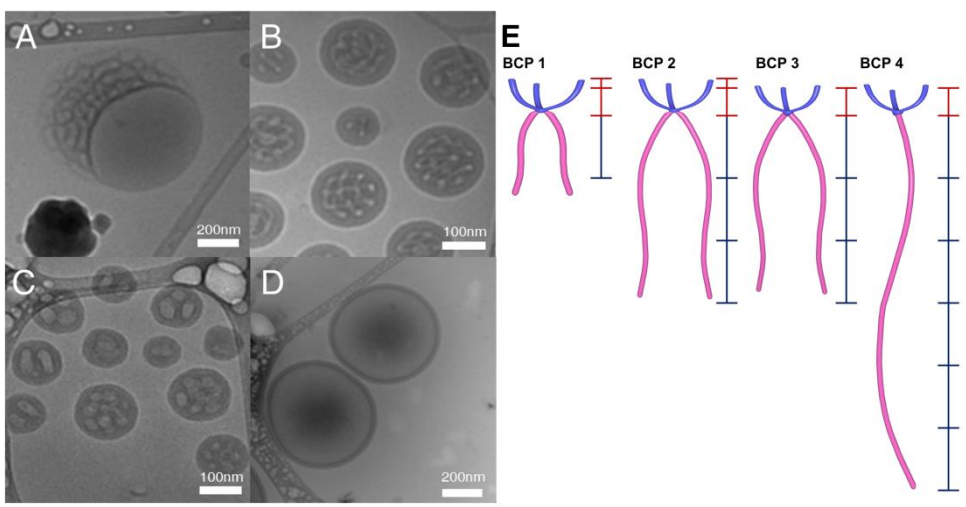


**Figure 10.** A-D) Cryo-TEM images of (A) **BCP 1**; acorn like structure, (B) **BCP 2**; hexagonal structure, (C) **BCP 3**; multi porous structure, and (D) **BCP 4**; vesicular structure. (E) Schematic illustration of **BCP 1-4**.

I simply compared critical packing parameter value $P = V/al$ of each BCP considered GPC $M_n$ value as volume of PI block $V$, product of backbone C-C bond number and length as $l$. Area of hydrophilic PEG '$a$' was simply assumed that $PEG750_3$ was relatively larger than $PEG550_3$.

Self-assembled structure of **BCP 1** was observed like ‘Acorn structure’ (Figure 10A). In lipid assembly, regular structures such as lipid cubosome showed some vesicles attached at the edges of the structure.[30-32] In polymer assembly, there were relatively disordered structure at the edge of the structure compared to the core. Enthalpy penalty was occurred at the curvature of the edge, which conflicted with the cubic structure. For overcoming the enthalpy penalty, disorder of the structure was formed in the direction of increasing entropy. The **BCP 1** was in a time of transition to make regular structure. At one side, organizing structure formed. At the other side, a big vesicle formed to overcome enthalpy change. If the assembled structure was small, the curvature angle was big. It means the enthalpy increase more than large structure. Then disorder of the structure increased more. Compared to PEG-*b*-PS, PEG-*b*-PI system made small first assembled unit having large curvature, so that bigger disorder of the structure formed.

The phase of the **BCP 2** was inverse hexagonal phase (Figure 10B). Compared to **BCP 2**, **BCP 3** had a smaller molecular weight of hydrophilic domain and similar hydrophobic domain. The contour length and volume of hydrophobic domain is same. However, the area of hydrophilic domain decreased, and the *P* value of **BCP 3** increased in comparison with **BCP 2**. The morphology of **BCP 3** was multi porous colloid (Figure 10C) which was made up of inverse micelle. Inverse micelle phase was observed above the *P* value of inverse hexagonal phase. Compared to **BCP 3**, **BCP 4** had the same molecular weight of hydrophilic domain and hydrophobic domain. However, the architecture was dendritic-linear shape, that hydrophobic domain had a linear structure, different from the dendritic-dendritic shape of

**BCP 3**. The dendritic-linear **BCP 4** structure had longer hydrophobic contour length while having same volume of hydrophobic blocks having same molecular weight. Thus, the *P* value of **BCP 4** decreased. As a result, **BCP 4** showed vesicle structure (Figure 10D) that was observed under 1 of *P* value.

## Cross-linking of PEG-*b*-PI.

**Table 3**. Derived count rates [x$10^3$kcps]

| | No Crosslinking | Photo initiator | | | |
|---|---|---|---|---|---|
| | | 3hr | | Overnight (17hr) | |
| | | Irgacure 2959 | Irgacure 651 | Irgacure 2959 | Irgacure 651 |
| **Water** | 673.33 | 515 | 756.6 | 332.3 | 348 |
| **THF** | 1.27 | 30.77 | 108.6 | 35.66 | 33.8 |
| **Relative count rates THF/Water (%)** | 0.18% | 5.97% | 14.35% | 10.73% | 9.71% |

* Crosslinking test using **BCP 5** polymer. Derived count rates mean scattered light intensity during the DLS measurement.

For radical cross-linking, I used photo radical generation. Water-soluble photoinitiator Irgacure2959 and hydrophobic photoinitiator Irgacure651 were compared. The concentration of polymer in solution assembly was 0.5wt%. Photoinitiator was added in a same weight amount as the polymer. Molar ratio of initiator was 100 eq. excess to the BCP and 0.3 eq. to the number of double bond in a BCP. UV light ($\lambda$=365nm, 15W) was irradiated for 3 hr and 17 hr (Table 3). The cross-linking of the double bond within the hydrophobic domains of **BCP 5** by photo radical generation was confirmed by changing the dispersion medium from water to THF. The non-cross-linked BCP structures were completely disassembled into individual

BCPs in THF, as evidenced by the drastic decrease in the scattered light intensity during the DLS measurement.[33] The cross-linked dispersions irradiated with UV light showed scattering in the DLS experiment after replacing the solvent to THF. Depending on the relative scattering intensity of the solvent, the cross-linking efficiency can be determined (Table 3). When the UV light was irradiated for 3 hr, the relative count rates of Irgacure2959 was under 10%. On the other hand, Irgacure651 was more effective than Irgacure2959, 14.35%. It resulted from the fact that hydrophobic Irgacure651 readily penetrated the hydrophobic domain having double bonds. In case of Irgacure2959, generated radicals were dissipated in water medium before embedding to hydrophobic domain. After irradiation for 17 hr, Irgacure2959 showed 10.73% of relative count rates. It was effective than 3hr irradiation, because longer irradiation time made times for radical diffusion into the hydrophobic domain. In case of Irgacure651, it showed 9.51% lower than 3hr irradiation. Collectively, cross-linking condition using the Irgacure651 and 365nm UV light irradiation for 3 hr was most efficient.

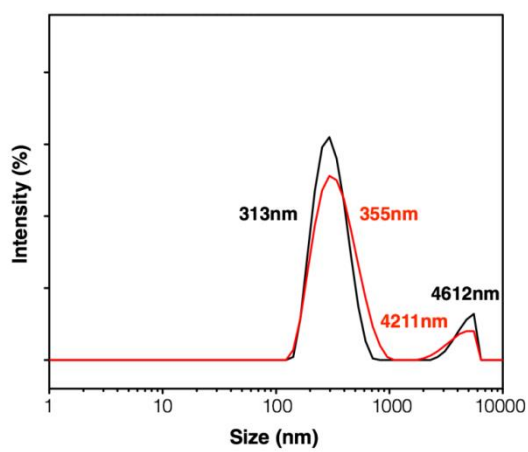


**Figure 11.** Dynamic light scattering (DLS) data of cross-linked assembled

**BCP 5** in water medium(Black) and THF medium(Red).

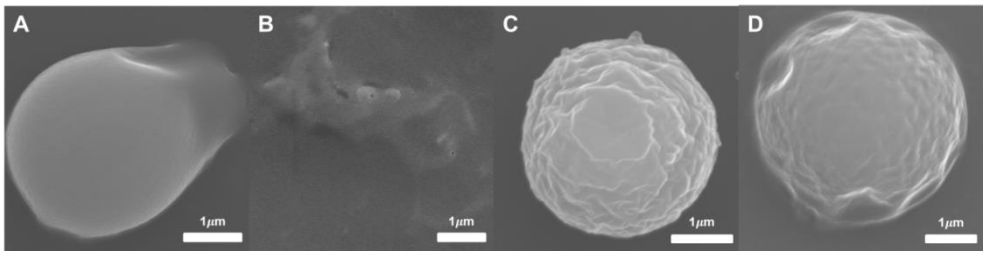


**Figure 12.** A-D) SEM images of assembled **BCP 5** polymer (A) before cross-linking in water, (B) in THF, (C) after cross-linking in water and (D) in THF.

The hydrodynamic diameter of the cross-linked polymer vesicles in THF was slightly larger than that in water, suggesting that the self-assembled vesicle structures swelled in THF (Figure 11). However, the more constructive structure, which was larger than 3μm diameter, was not swollen well in THF. The change of the structural maintenance of the BCP after cross-linking was visualized by SEM (Figure 12). Before cross-linking, a melted edge of the assembled structure was observed in a water medium. Changing the medium to THF, there was no more structure. On the other hand, after cross-linking, assembled structures were observed well without edge melting in both water and THF medium. It means that cross-linking was effective to preserve the assembled structure of BCPs which has low $T_g$.

In case of film cross-linking, 0.03eq. of Irgacure651 to the number of double bonds in a BCP was added. The film was made by the ‘solvent diffusion-evaporation mediated self-assembly’ (SDEMS) procedure.[34] The dioxane solution of BCP (12.5wt%) and photoinitiator cast on a glass

substrate was placed in a sealed humidity chamber (Dioxane : Water = 50 : 50). After 4 hr, the glass substrate was moved to 100% water humidity chamber and cured by same 365nm UV light lamp for 17hr. Cured glass substrate was immersed into water 1 day and dried on the filter paper.

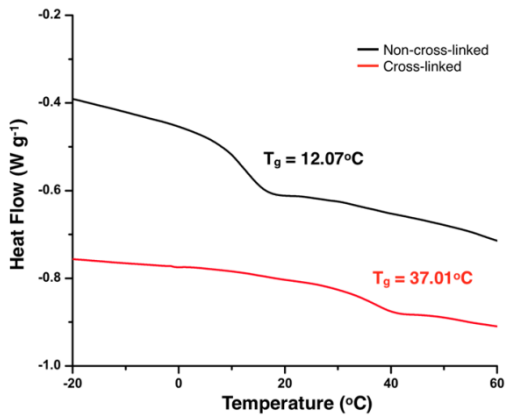


**Figure 13.** Differential scanning calorimetry (DSC) analysis of non-cross-linked **BCP 5** and cross-linked **BCP 5** film obtained at 5 ℃ min$^{-1}$ heating rate.

For the thicker structure of film compared to the solution assembled structure, 365nm UV light was irradiated 17 hr. The cross-linking of the film was confirmed by $T_g$ increase. $T_g$ was measured by DSC from -50 ℃ to 200℃ at 5 ℃ min$^{-1}$ heating rate (Figure 13). After cross-linking, $T_g$ increased about 25 ℃ from 12.07 ℃ to 37.01 ℃. Cross-linking between polymer chains decreased the mobility of the polymer, so that $T_g$ increased.

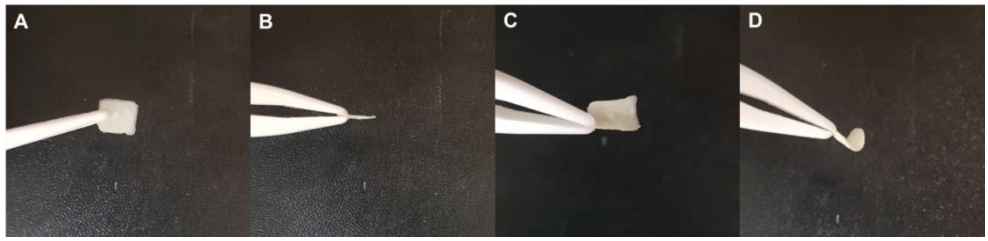


**Figure 14.** A-D) Photo images of BCP_PI-2 **BCP 5** polymer film after crosslinking. (A, B) Before bending. (C, D) After bending.

Crosslinking was also visually checked. The film was bent and twisted by the artificial forces. As a result, the film shape was transformed, but not broken (Figure 14). Polyisoprene made film flexible, so that film was not crashed or broken by the external forces.

# 3. Conclusion

In conclusion, I developed highly acetylene functionalized polyisoprene through anionic polymerization using a synthesized alkyl lithium initiator. Click chemistry was an efficient way to synthesize the dendritic block copolymers by coupling the hydrophilic PEG domain and the hydrophobic PI domain. As changes were made to structural factors such as molecular weight, contour length and shape, the critical packing parameter value of BCPs changed. As a result, I observed various structures which were generated by solution self-assembly of BCPs through cryo-TEM. Furthermore, cross-linking of hydrophobic domain using photochemically induced radical coupling was effective in maintaining the assembled BCP structures. The rubbery PI hydrophobic domain enhanced the mechanical properties of the BCP compared to the BCP with PS as a hydrophobic domain.

# 4. Experimental and Supporting information

## Materials.

All reagents and chemicals were used as received unless otherwise noted. Isoprene monomer was stirred over $CaH_2$ for 24 hr, transferred to clean schlenk RBF by vacuum distillation. $CH_2Cl_2$ and Cyclohexane was dried (using $CaH_2$ under $N_2$ atmosphere) and distilled. Tetrahydrofuran (THF) was refluxed with sodium and benzophenone under $N_2$ atmosphere and distilled before use. All reactions were performed in an inert atmosphere unless otherwise noted.

## Methods.

$^{1}H$ NMR and $^{13}C$ NMR spectra were recorded by Agilent 400-MR DD2 Magnetic Resonance System and Varian/Oxford As-500 using $CD_2Cl_2$ and $CDCl_3$ as solvents and internal standards. Molecular weights and polydispersity indices of polymers and block copolymers were measured by Agilent 1260 Infinity gel permeation chromatography (GPC) system equipped with a PL gel 5 μm MiniMIX-D column (Agilent Technologies) and differential refractive index detectors. THF was used as an eluent with a flow rate of 0.3 mL $min^{-1}$ at 35 ℃. A PS standard kit (Agilent Technologies) was used for calibration. Cryogenic transmission electron microscopy (cryo-TEM) images were taken from JEM-1400 (JEOL, Japan) operating at 120 kV. The cryo-TEM experiments were performed with a thin film of aqueous sample solution (5 $\mu$L) transferred to a lacey supported grid by the plunge-dipping method. The thin aqueous films were

prepared at ambient temperature and with a humidity of 97-99% within a custom-built environmental chamber in order to prevent water evaporation from the sample solution. The excess liquid was blotted with filter paper for 1-2 sec, and the thin aqueous films were rapidly vitrified by plunging them into liquid ethane (cooled by liquid nitrogen) at its freezing point. Scanning electron microscopy (SEM) was performed on a Hitachi S-4300 operating at 15 kV. Suspension was cast and dried on a slide glass, and coated with Pt by using a Hitachi E-1030 ion sputter. Dynamic light scattering (DLS) was performed at a Malvern Zetasizer Nano-S. Fourier transform infrared spectrophotometer (FT-IR) was measured on SHIMADZU IR Tracer-100 equipped with MIRacle 10 single reflection ATR accessory. Differential scanning calorimetry (DSC) was carried out under $N_2$ gas at a scan rate of 5 ℃ $min^{-1}$ with TA Instruments Q10.

## Synthesis of hydrophilic modules [28, 29]

**PEG750-OTs (A1)**

Monomethoxy PEG (30g, Mn = 750 g/mol) and triethylamine (10.12 g, 0.1 mol) were dissolved in dry dichloromethane (MC) (150 mL). Tosyl chloride (19 g, 0.1 mol) in 100mL dry MC added dropwise into the PEG solution at 0 ℃. The solution was stirred for 24 hr at room temperature. The solution was quenched and extracted with 1M HCl solution several times. The organic layer was dried with $MgSO_4$ and evaporated on a rotary evaporator. The crude product was purified by column chromatography using MC as an eluent. The compound was yellow solid-liquid. Yield 29g

(77.65%) **$^{1}$H NMR** (400 MHz, $CDCl_3$) 7.78(d, J=5.1 Hz, 2H), 7.32(d, J=5.7 Hz, 2H), 4.13(t, J=5.1 Hz, 2H), 3.68-3.31 (m, -$CH_2CH_2O$-), 3.36(s, 3H), 2.43(s, 3H)

**PEG750$_3$-benzoate (A2)**

**A1** (25g, 0.027mol), Potassium carbonate (40.30g 0.28mol), and Methyl-3,4,5-trihydroxy benzoate (1.46g, 0.08mol) were dissolved in acetone (500ml) at two neck flask. Flask was equipped with reflux line. Reaction was refluxed 2 days at 70 ℃. Reaction was traced by GPC and MALDI-TOF. The solution was evaporated on a rotary evaporator and the resulting residue was redissolved in MC, which was then extracted with 1M HCl solution several times. The organic layer was evaporated on a rotary evaporator. **MALDI-TOF** Mn = 2339.41 g mol‑1 .

**PEG750$_3$-benzyl alcohol(A3)**

**A2** (20.5g, 0.0086mol) was dissolved in dry tetrahydrofuran (THF). The solution was slowly dropped into the $LiAlH_4$ (0.81g 0.0214mol) in dry THF solution at ice bath. The solution was stirred 4hr from 0 ℃ to room temperature. The reaction was quenched with few drops of water and 1M NaOH solution. Then, the solution was filtered, dried with $MgSO_4$, and evaporated on a rotary evaporator. The crude product was purified by column chromatography using MC and methanol (MeOH) as an eluent. The compound was yellow solid-liquid. **$^{1}$H NMR** (400 MHz, $CDCl_3$) 6.64(s, 2H), 4.58(d, J=5.6 Hz, 2H), 4.18(t, J=5.2 Hz, 4H), 4.14(t, J=5.2 Hz, 2H), 3.93-3.45 (m, -$CH_2CH_2O$-), 3.39(s, 9H), 2.52(t, J=5.6 Hz, 1H); **$^{13}$C NMR** (400 MHz, $CDCl_3$) 152.60, 137.49,137.22, 106.50, 72.29, 71.95, 70.77-

70.57, 69.83, 68.79, 64.86, 59.07; **GPC** Mn = 3190 g mol-1 , Đ =1.03; **MALDI-TOF** Mn = 2411.34 g mol-1 .

**PEG750$_3$-benzyl chloride(A4)**

**A3** (6g, 0.0025mol) was dissolved in dry MC. $SOCl_2$ (0.06g, 0.0050mol) was slowly dropped into the solution at ice bath. The solution was stirred 4hr from 0 ℃ to room temperature. The reaction was quenched by extraction with saturated $NaHCO_3$ solution. Then, the organic layer was dried with $MgSO_4$, and evaporated on a rotary evaporator. The compound was yellow solid-liquid. **$^1$H NMR** (400 MHz, $CDCl_3$) 6.62(s, 2H), 4.46(d, J=5.6 Hz, 2H), 4.16(m, J=5.2 Hz, 4H), 4.13(m, J=5.2 Hz, 2H), 3.93-3.45 (m, -$CH_2CH_2O$-), 3.38(s, 9H).

**Synthesis of PEG750$_3$-azide(A5)**

**A4** (5g, 0.0021mol) and 10eq of $NaN_3$ (1.36g, 0.021mol) were added into dimethylformamide (DMF) (50ml). The solution was stirred for overnight at room temperature. The solvents were removed under reduced pressure and diluted with MC and then extracted with water. The organic layer was dried with $MgSO_4$; the solvents were removed under reduced pressure. The compound was yellow solid-liquid. **$^1$H NMR** (400 MHz, $CDCl_3$) 6.54(s, 2H), 4.24(d, J=5.6 Hz, 2H), 4.16(m, J=5.2 Hz, 4H), 4.13(m, J=5.2 Hz, 2H), 3.93-3.45 (m, -$CH_2CH_2O$-), 3.38(s, 9H).

**Methyl 3,5-dimethylbenzoate(B1)**

A few drops of $H_2SO_4$ (95.0 %) were added into methyl 3,5-dimethylbenzoic acid (10g, 0.066 mol) in methanol (100ml). The solution was refluxed at 70 ℃ for 10 hr. The reaction mixture was quenched with ice and extracted with ether. The organic layer was washed with $Na_2CO_3$ saturated solution and dried over $MgSO_4$; the solvents were removed under reduced pressure. The crude product was purified by column chromatography using n-hexane as an eluent. The compound (**B1**) was obtained as colorless oil. Yield 9.8g (89.63%) **$^1$H NMR** (400 MHz, $CDCl_3$) 7.66 (s, 2H), 7.19 (s, 1H), 3.90 (s, 3H), 2.36 (s, 6H).

**Methyl 3,5-bis(bromomethyl)benzoate(B2)**

**B1** (5.8g, 35.323 mmol) and N-Bromosuccinimide (13.83g, 0.077 mmol, 2.2eq.) were added into benzene (250ml). The solution was degassed by bubbling $N_2$ for 15 min. Azobisisobutyronitrile (0.58g, 3.532 mmol, 0.1 eq.) was added into the solution and stirred at 95 ℃ for 12 hr. The precipitate was filtered off and washed with hot benzene. The combined filtrate was washed with $NaHCO_3$ saturated solution and brine. The residue was dried with $MgSO_4$; the solvents were removed under reduced pressure. The crude product was purified by column chromatography using hexane as an eluent. Yield 3.33g (30.61%) **$^1$H NMR** (400 MHz, $CDCl_3$) 8.00 (s, 2H), 7.62 (s, 1H), 4.50 (s, 4H), 3.93(s, 3H).

**Methyl 3,5-bis(azidomethyl)benzoate(B3)**

**B2** (3.33g, 10.34 mmol) and $NaN_3$ (2.68g, 41.366 mmol, 4 eq.) were added into DMF (50ml). The solution was stirred at 65 ℃ for 3 hr. It was

diluted with water and then extracted with ethyl acetate (EA). The organic layer was dried with $MgSO_4$; the solvents were removed under reduced pressure. The crude product was purified by column chromatography using hexane as an eluent. Recrystallization in hexane gave a white crystalline solid. Yield 2.23g (87.57%) **$^1$H NMR** (400 MHz, $CDCl_3$): 7.97 (s, 2H), 7.49 (s, 1H), 4.49 (s, 4H), 3.95 (s, 3H).

**Methyl 3,5-bis(azidomethyl)benzoic acid(B4)**

A solution of 2M LiOH (10ml) was added into **B3** (1g, 4.061 mmol) in methanol (70ml). The reaction was stirred at room temperature for 12 hr. The solvents were removed under reduced pressure and monitored by TLC. Then, 2M HCl solution was added into the mixture until pH was dropped to pH 5-6. Mixture was extracted with EA and brine, and then dried with $MgSO_4$; the solvents were removed under reduced pressure. A white solid was collected. Yield 0.91g (71.95%) **$^1$H NMR** (400 MHz, $CDCl_3$) 8.04(s, 2H), 7.56(s, 1H), 4.49(s, 16.5MHz, 4H).

**Synthesis of PEG750$_3$-bisazide (C1)**

**B4 (Methyl 3,5-bis(azidomethyl)benzoic acid)** (0.475 g, 1.54 mmol, 5.2 eq.), N,N'-dicyclohexylcarbodiimide (0.367 g, 1.78 mmol, 6 eq.), and 4-dimethylaminopyridine (0.0072 g, 0.059 mmol, 0.2 eq.) were dissolved in dry MC (50 mL) at 0 ℃. The mixture was slowly added to the MC solution (50 mL) of **A3 (PEG750$_3$-OH)** (0.7g, 0.297 mmol, 1 eq.) at 0 ℃. The resulting mixture was gradually warmed to room temperature. After 24 hr, the crude mixture was cooled, and urea was removed by recrystallization in cold EA. Then mixture was purified by flash column chromatography using

silica gel (dichloromethane : methanol = 95:5 v/v). **$^1$H NMR** (400 MHz, $CDCl_3$) 8.00(s, 2H), 7.50(s, 1H), 6.68(s, 2H), 5.25(s, 2H), 4.45(s, 4H), 3.93-3.45 (m, -$CH_2CH_2O$-), 3.38(s, 9H); **GPC** Mn = 3060 g $mol^{-1}$ , Đ =1.04

# Synthesis of hydrophobic modules

**Synthesis of the initiator 5-triethylsilyl-4-pentynyllithium (TESPLi)**[24]

A 10-fold excess of lithium (0.8g, 0.11mol) over the (5-chloro-1-pentynyl)triethylsilane (TESP-Cl) (2.5g, 0.011mol) was used. Dry cyclohexane (50ml) was added to the lithium placed in 100ml two neck flask with condenser under an argon atmosphere. Lithium was stirred vigorously for 30min at 50 ℃. Then, TESPCl was added dropwise and stirred for 4hr at 50 ℃ and overnight at room temperature. The solution was filtered using fine porous schlenk filter funnel and led to transparent vivid red-orange solution. **$^1$H NMR** (400 MHz, $CDCl_3$) 2.15(t, 2H), 1.45(m, 2H), 0.97-0.82(m, 12H), 0.49(m, 6H).

**Polymerization of α-Acetylene-Functionalized Polyisoprene.**

All polymerization were performed in flame dried glass apparatus. Isoprene monomer was stirred over $CaH_2$ for 24 hr, transferred by vacuum distillation into a clean flask. Amount of isoprene monomer was added to a dry cyclohexane in a schlenk flask and degassed for 20min. The solution temperature was increased until 33-35 ℃. Then, synthesized **TESPLi** was introduced to the monomer solution. The polymerization progress was

monitored using GPC at 30min intervals. After 2h, the reaction was almost done and quenched by injecting methanol. The solution was evaporated under reduce pressure and precipitated into methanol for 3 times. Colorless viscous product (**Pro_PI**) was obtained after drying. Then, the product and tetrabutylammonium fluoride trihydrate (TBAF) (5 equiv. of **Pro_PI** ) were dissolved in THF and stirred at ambient condition for 4 h. Then, the solution was precipitated in methanol and dried. Colorless viscous product (**Depro_PI**) was obtained. In case of 1,2-addition, polymerization was going under -78 ℃. **$^1$H NMR** (400 MHz, $CDCl_3$) 6.1-5.5(1,2, -CH-), 5.10(1,4, -CH-), 4.8-1.6(1,2, -$CH_2$), 4.75 (3,4, -$CH_2$), 2.03(1,4, -$CH_2$-), 2.0(3,4, -CH-), 2.0-1.8(1,4, -$CH_2$-), 1.8-1.2(1,2, -$CH_2$), 1.65(1,4, -$CH_3$), 1.64(3,4, -$CH_3$), 1.36(3,4, -$CH_2$-), 1.15-1.0(1,2, -$CH_3$).[35]

**Synthesis of block copolymers by click chemistry**

CuBr (I) (40 mg) was dried in vacuum for 15 min. N,N,N',N'',N''-Pentamethyldiethylenetriamine (PMDETA) (80 mg) mixed with THF (1.5 mL) was added and the mixture was stirred in $N_2$ for 15 min. To this solution, a solution of **PEG750$_3$-bisazide** (0.05 g, 0.08 mmol) and **α-Acetylene-Functionalized Polyisoprene** (4 eq. of **PEG750$_3$-bisazide**) in THF(5 mL) was added. The mixture was degassed by bubbling $N_2$ for 15 min. After degassing, the click reaction was proceeded at 40 ℃ until completion. The extent of the reaction was monitored by GPC. The reaction was quenched by exposing the solution to the air, followed by dilution with chloroform. The cooled solution was filtered through a pack of aluminum oxide (basic) with $CHCl_3$ to remove the Cu catalyst. The filtered solution was concentrated on a rotary evaporator, and then crude products were

dissolved in a small amount of dichloromethane and precipitated into methanol. Colorless viscous liquid was collected by dried in vacuum. The crude mixture was further purified by flash column chromatography ($SiO_2$, $CH_2Cl_2$) to remove excess homo PI, and, if necessary, by preparatory size exclusion chromatography.

Same click reaction procedure for dendritic-linear PEG-*b*-PI

# Supporting information (Spectra)

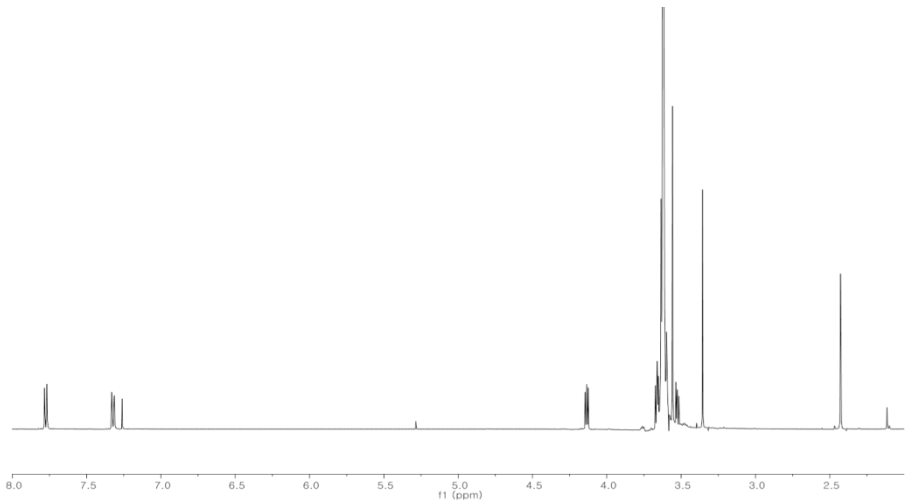


$^1$H NMR spectra of PEG750-Ts (A1) ($CDCl_3$)

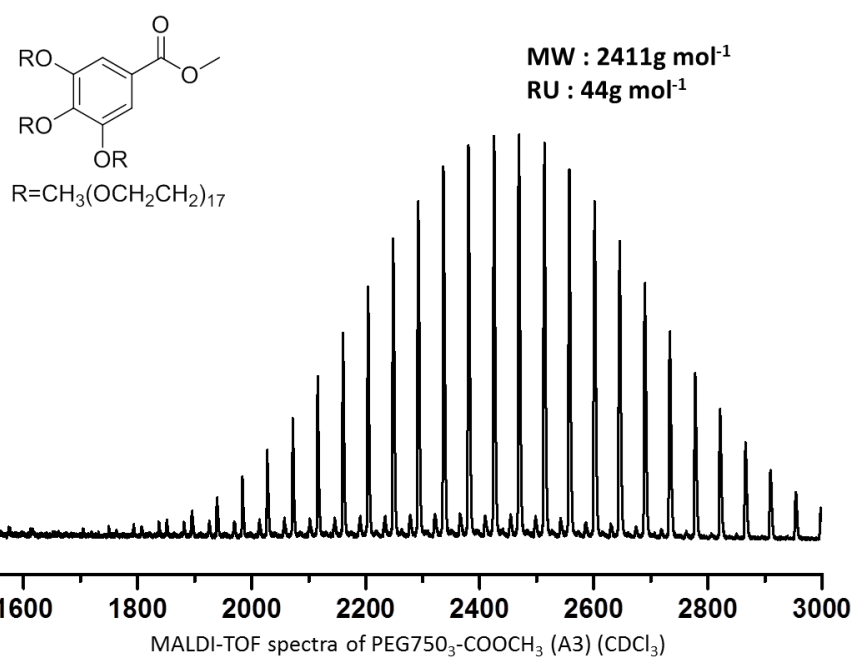


MALDI-TOF spectra of $PEG750_3$-$COOCH_3$ (A3) ($CDCl_3$)

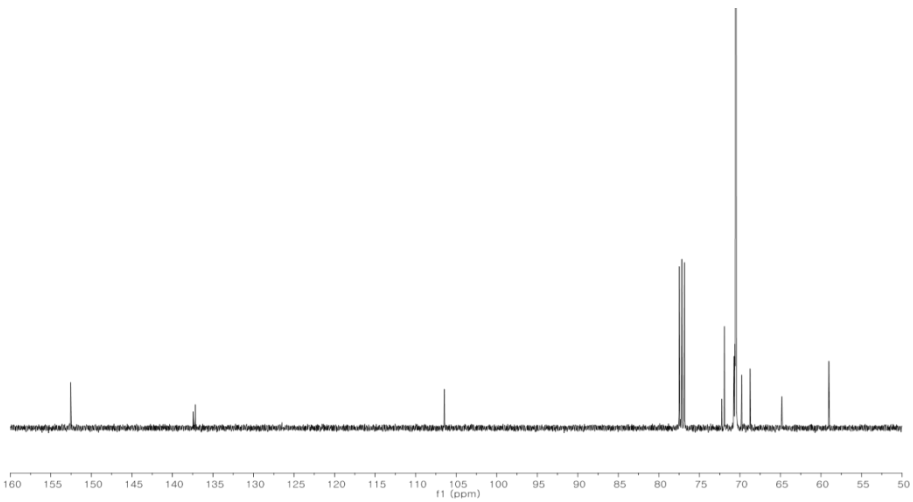


$^{13}$C NMR spectra of PEG750$_3$-OH (A3) ($CDCl_3$)

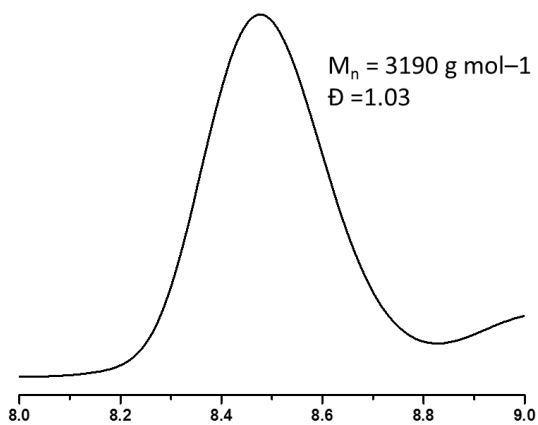


GPC spectra of PEG750$_3$-OH (A3) ($CDCl_3$)

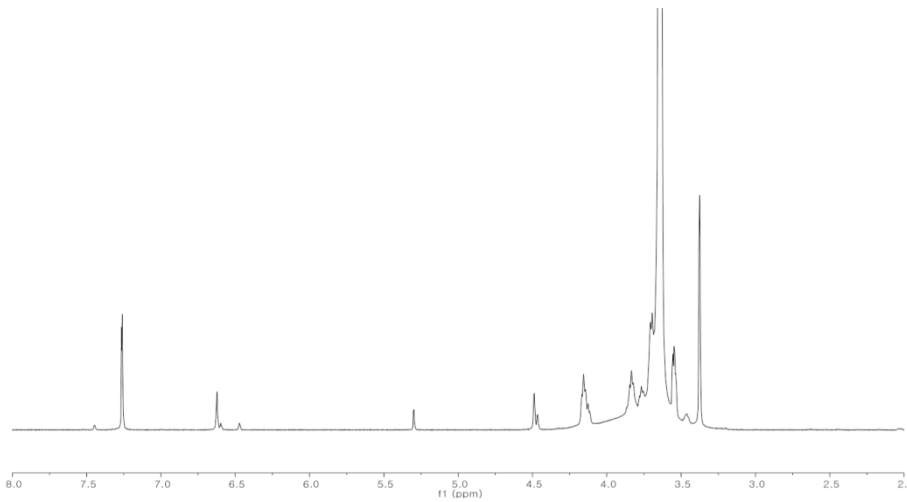


$^1$H NMR spectra of PEG750$_3$-Cl (A4) ($CDCl_3$)

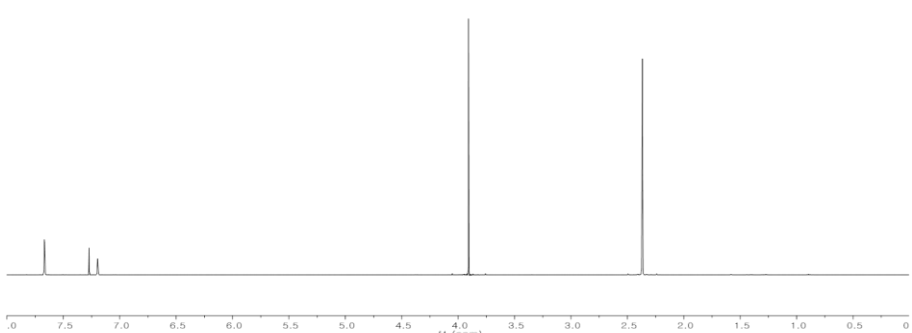


$^1$H NMR spectra of Methyl 3,5-dimethylbenzoate (B1) ($CDCl_3$)

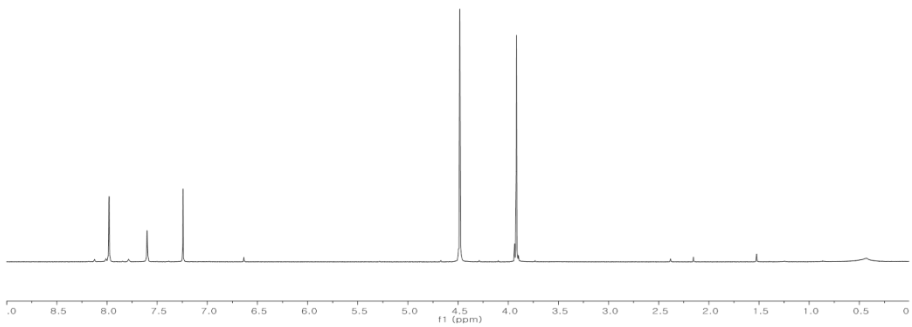


$^1$H NMR spectra of Methyl 3,5-bis(bromomethyl)benzoate (B2) ($CDCl_3$)

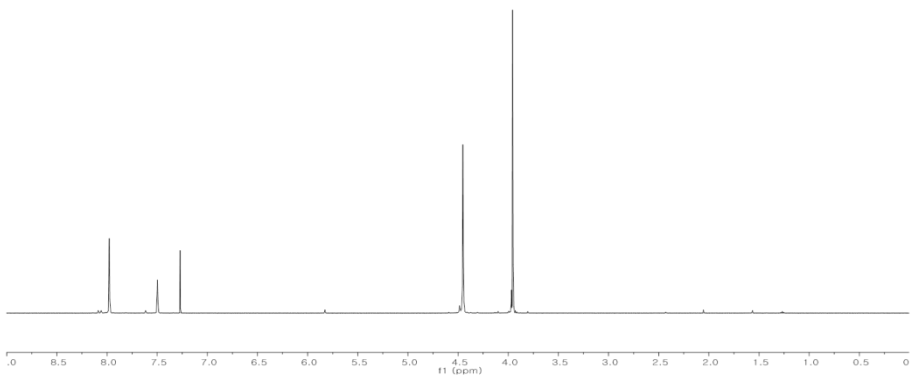


$^1$H NMR spectra of Methyl 3,5-bis(azidomethyl)benzoate (B3) ($CDCl_3$)

# References

1. J. N. Israelachvili, *Intermolecular and surface forces*. Academic press: 2011.

2. J. N. Israelachvili, D. J. Mitchell, B. W. Ninham, Theory of self-assembly of hydrocarbon amphiphiles into micelles and bilayers. *Journal of the Chemical Society, Faraday Transactions 2: Molecular and Chemical Physics* **1976,** *72*, 1525-1568.

3. L. Zhang, A. Eisenberg, Multiple Morphologies of "Crew-Cut" Aggregates of Polystyrene-*b*-poly(acrylic acid) Block Copolymers. *Science* **1995,** *268* (5218), 1728-31.

4. J. C. van Hest, D. A. Delnoye, M. W. Baars, M. H. van Genderen, E. W. Meijer, Polystyrene-dendrimer amphiphilic block copolymers with a generation-dependent aggregation. *Science***1995,** *268* (5217), 1592-5.

5. D. E. Discher, A. Eisenberg, Polymer vesicles. *Science* **2002,** *297* (5583), 967-973.

6. G. H. Fredrickson, L. Leibler, Theory of block copolymer solutions: nonselective good solvents. *Macromolecules* **1989,** *22* (3), 1238-1250.

7. U. Tritschler, S. Pearce, J. Gwyther, G. R. Whittell, I. Manners, 50th Anniversary Perspective: Functional Nanoparticles from the Solution Self-Assembly of Block Copolymers. *Macromolecules* **2017,** *50* (9), 3439-3463.

8. R. K. O'Reilly, C. J. Hawker, K. L. Wooley, Cross-linked block copolymer micelles: functional nanostructures of great potential and versatility. *Chem Soc Rev* **2006,** *35* (11), 1068-83.

9. Y. Mai, A. Eisenberg, Self-assembly of block copolymers. *Chem Soc Rev*

**2012,** *41* (18), 5969-85.

10. Y. La, C. Park, T. J. Shin, S. H. Joo, S. Kang, K. T. Kim, Colloidal inverse bicontinuous cubic membranes of block copolymers with tunable surface functional groups. *Nat Chem* **2014,** *6* (6), 534-41.

11. T. H. An, Y. La, A. Cho, M. G. Jeong, T. J. Shin, C. Park, K. T. Kim, Solution self-assembly of block copolymers containing a branched hydrophilic block into inverse bicontinuous cubic mesophases. *ACS Nano* **2015,** *9* (3), 3084-96.

12. Y. La, T. H. An, T. J. Shin, C. Park, K. T. Kim, A Morphological Transition of Inverse Mesophases of a Branched-Linear Block Copolymer Guided by Using Cosolvents. *Angew. Chem. Int. Ed. Engl.* **2015,** *54* (36), 10483-7.

13. A. Cho, Y. La, T. J. Shin, C. Park, K. T. Kim, Structural Requirements of Block Copolymers for Self-Assembly into Inverse Bicontinuous Cubic Mesophases in Solution. *Macromolecules* **2016,** *49* (12), 4510-4519.

14. A. Cho, Y. La, S. Jeoung, H. R. Moon, J.-H. Ryu, T. J. Shin, K. T. Kim, Mix-and-Match Assembly of Block Copolymer Blends in Solution. *Macromolecules* **2017,** *50* (8), 3234-3243.

15. N. S. Cameron, M. K. Corbierre, A. Eisenberg, Asymmetric amphiphilic block copolymers in solution: a morphological wonderland. *Can. J. Chem.* **1999,** *77* (8), 1311-1326.

16. S. J. Holder, G. Woodward, B. McKenzie, N. A. Sommerdijk, Semi-crystalline block copolymer bicontinuous nanospheres for thermoresponsive controlled release. *RSC Advances* **2014,** *4* (50), 26354-26358.

17. B. E. McKenzie, H. Friedrich, M. J. Wirix, J. F. de Visser, O. R. Monaghan, P. H. Bomans, F. Nudelman, S. J. Holder, N. A. Sommerdijk,

Controlling internal pore sizes in bicontinuous polymeric nanospheres. *Angew. Chem. Int. Ed.* **2015,** *54* (8), 2457-2461.

18. B. E. McKenzie, F. Nudelman, P. H. Bomans, S. J. Holder, N. A. Sommerdijk, Temperature-responsive nanospheres with bicontinuous internal structures from a semicrystalline amphiphilic block copolymer. *J. Am. Chem. Soc.* **2010,** *132* (30), 10256-10259.

19. W. A. Phillip, R. M. Dorin, J. Werner, E. M. Hoek, U. Wiesner, M. Elimelech, Tuning structure and properties of graded triblock terpolymer-based mesoporous and hybrid films. *Nano Lett* **2011,** *11* (7), 2892-900.

20. Y. Y. Won, K. Paso, H. T. Davis, F. S. Bates, Comparison of Original and Cross-linked Wormlike Micelles of Poly(ethylene oxide-b-butadiene) in Water: Rheological Properties and Effects of Poly(ethylene oxide) Addition. *The Journal of Physical Chemistry B* **2001,** *105* (35), 8302-8311.

21. C. Decker, T. N. T. Viet, Photocrosslinking of functionalized rubbers, 7. Styrene-butadiene block copolymers. *Macromolecular Chemistry and Physics* **1999,** *200* (2), 358-367.

22. M. Morton, E. E. Bostick, R. A. Livigni, L. J. Fetters, Homogeneous anionic polymerization. IV. Kinetics of butadiene and isoprene polymerization with butyllithium. *J. Polym. Sci. Part A: General Papers* **1963,** *1* (5), 1735-1747.

23. D. J. Worsfold, S. Bywater, Anionic Polymerization of Isoprene. *Can. J. Chem.* **1964,** *42* (12), 2884-2892.

24. A. Touris, J. W. Mays, N. Hadjichristidis, Acetylene-Functionalized Lithium Initiators for Anionic Polymerization. Powerful Precursors for "Click" Chemistry. *Macromolecules* **2011,** *44* (7), 1886-1893.

25. S. Bywater, D. J. Worsfold, Anionic Polymerization of Styrene Effect of

Tetrahydrofuran. *Can. J. Chem.* **1962,** *40* (8), 1564-1570.

26. H. Hsieh, R. P. Quirk, *Anionic polymerization: principles and practical applications*. CRC Press: 1996.

27. R. Faust, J. P. Kennedy, Living carbocationic polymerization. *Polymer Bulletin* **1986,** *15* (4).

28. M. Maldovan, E. L. Thomas, Diamond-structured photonic crystals. *Nat Mater* **2004,** *3* (9), 593-600.

29. M. G. Jeong, J. C. van Hest, K. T. Kim, Self-assembly of dendritic-linear block copolymers with fixed molecular weight and block ratio. *Chem Commun (Camb)* **2012,** *48* (30), 3590-2.

30. R. Efrat, E. Kesselman, A. Aserin, N. Garti, D. Danino, Solubilization of hydrophobic guest molecules in the monoolein discontinuous QL cubic mesophase and its soft nanoparticles. *Langmuir* **2009,** *25* (3), 1316-26.

31. D. Demurtas, P. Guichard, I. Martiel, R. Mezzenga, C. Hebert, L. Sagalowicz, Direct visualization of dispersed lipid bicontinuous cubic phases by cryo-electron tomography. *Nat Commun* **2015,** *6*, 8915.

32. J. Gustafsson, H. Ljusberg-Wahren, M. Almgren, K. Larsson, Submicron particles of reversed lipid phases in water stabilized by a nonionic amphiphilic polymer. *Langmuir* **1997,** *13* (26), 6964-6971.

33. M. G. Jeong, K. T. Kim, Covalent Stabilization of Inverse Bicontinuous Cubic Structures of Block Copolymer Bilayers by Photodimerization of Indene Pendant Groups of Polystyrene Hydrophobic Blocks. *Macromolecules* **2016,** *50* (1), 223-234.

34. C. Park, Y. La, T. H. An, H. Y. Jeong, S. Kang, S. H. Joo, H. Ahn, T. J. Shin, K. T. Kim, Mesoporous monoliths of inverse bicontinuous cubic phases of block copolymer bilayers. *Nat commun* **2015,** *6*, 6392.

35. H. Sato, Y. Tanaka, 1H-NMR study of polyisoprenes. *Journal of Polymer Science: Polymer Chemistry Edition* **1979,** *17* (11), 3551-3558.

# 국문 초록

## 가교 가능한 폴리아이소프렌을 소수성 블록으로 갖는 블록 공중합체 연구

윤 미 선

화학부 고분자화학 전공

서울대학교 대학원

블록 공중합체란 두 개 또는 그 이상의 구분된 고분자 블록이 공유결합으로 연결된 거대 분자를 말한다. 블록 공중합체는 벌크 상이나 수용액 상에서 자기조립을 통해 다양하게 응용 가능한 정교한 나노 구조체를 만드는 물질로 주목 받고 있다. 수용액 상에서 블록 공중합체의 자기조립을 통해 만든 정교한 다공성 구조체는 고분자의 구조, 두 블록의 분자량 비, 그리고 조립조건에 의해 조절될 수 있다. 그러나 이렇게 만들어진 정교한 다공성 나노 구조체는 비 공유결합으로만 이루어져 극한 환경에서는 사용되지 못한다. 따라서, 자기 조립된 구조가 유기용매, 고온, 극한 pH 및 물리적 스트레스와 같은 극한 환경에서 견디려면 공유결합이 필요하다. 이 학위논문에서는 가지상의 친수성 폴리에틸렌글라이콜(PEG) 블록과 가지상의 소수성 폴리아이소프렌(PI) 블록으로 이루어진 블록 공중합체의 합성을 보여준다. PI는 유리전이온도가 낮고, 가교될 수 있는 반복단위를 갖고 있다. 이렇게 합성된 블록 공중합체의 구조와 블록의 비율이 수용액 상에서의 자기조립에 미치는 영향을 조사 했다. 자기 조립된 구조는

블록 공중합체의 PI의 가교에 의해 공유결합으로 안정되었으며 극한 환경에서 가교 후의 구조안정성도 확인하였다.

**주요어 :** 블록 공중합체, 폴리에틸렌글라이콜, 폴리아이소프렌, 수용액 상 자기조립, 가교, 나노구조

**학 번 :** 2016-20353